

Received March 22, 2019, accepted April 10, 2019, date of publication April 17, 2019, date of current version May 6, 2019.

Digital Object Identifier 10.1109/ACCESS.2019.2911702

An Ordered Curtailment Strategy for Offshore Wind Power Under Extreme Weather Conditions Considering the Resilience of the Grid

QI WANG¹, (Member, IEEE), ZHIPENG YU¹, RONG YE², ZHANGSUI LIN²,
AND YI TANG¹, (Senior Member, IEEE)

¹School of Electrical Engineering, Southeast University, Nanjing 210096, China

²State Grid Fujian Electric Power Co., Ltd., Economic Technology Research Institute, Fuzhou 350012, China

Corresponding author: Zhipeng Yu (yuzhipeng@seu.edu.cn)

This work was supported by the Science and Technology Project of State Grid Fujian Electric Power Co. (Research on Key Technologies for Efficient Delivery and Consumption of Offshore Wind Farm Groups).

ABSTRACT Typhoon is an important factor leading to offshore wind power ramp events, which can easily cause a serious imbalance between the supply and the demand, thus affecting the security and stability of the power system operation. First, based on the actual typhoon path, this paper analyzes its impact on the output characteristics of offshore wind farms and proposes a framework to mitigate the impact of wind power ramping. On this basis, an ordered curtailment strategy for large-scale offshore wind power systems, considering the resilience of the grid, is proposed. With the goals of system safety, stability and operational economy, wind power ramp data are utilized to optimize the ordered curtailment of offshore wind power, considering wind power curtailment, the adjustment ability of generators and the demand response. The simulation analysis of the IEEE-RTS24 node system shows that the proposed strategy can reduce the operating cost of the system while ensuring its security and stability.

INDEX TERMS Wind power ramping, security and stability of power system operation, grid resilience, ordered curtailment strategy for offshore wind power.

I. INTRODUCTION

Offshore wind power has developed rapidly in recent years [1], [2] due to characteristics such as high utilization hours and high-level, stable output [3]–[5]. Compared with onshore wind power, offshore wind power generations (OWPGs) are more susceptible to extreme weather [6], [7] (e.g., typhoons), causing wind power ramp-down events [8] and seriously threatening the safety and stability of power system operation. For traditional coal-fired thermal power unit-based power systems, due to ramp rate limitations, most systems cannot cope with wind power ramp-down events [9]–[11], making it more difficult to balance power supply and demand.

Current research on wind power ramp events mainly focuses on three aspects: wind power ramping prediction and identification [12], [13], ramping control at the wind farm side and ramping control using an energy storage system.

The associate editor coordinating the review of this manuscript and approving it for publication was Lorenzo Ciani.

(1) The time window selection [14], [15] for wind power prediction and the modeling of wind power ramp events using data modeling [16]–[18] and scene analysis [19] are the focuses of recent studies. These studies mainly concentrate on effectively predicting the occurrence of wind power ramp events.

(2) The utilization of power control at the wind farm side [20], [21] to suppress wind power ramping has achieved good results in practice. The ramp rate and the amount of abandoned wind are considered comprehensively to limit the wind power ramp rate at the high ramp rate stage and improve wind power accommodation at the low ramp rate stage, which can reduce the impact of wind power fluctuation on the system. The adjustment capability of this type of method is limited by the state of the wind farm itself and its current active power control capability. Therefore, the above method is a kind of finite control that may not be able to effectively control wind power ramping in some extreme cases.

(3) To address wind power ramp events more effectively, the joint optimization of wind power and energy

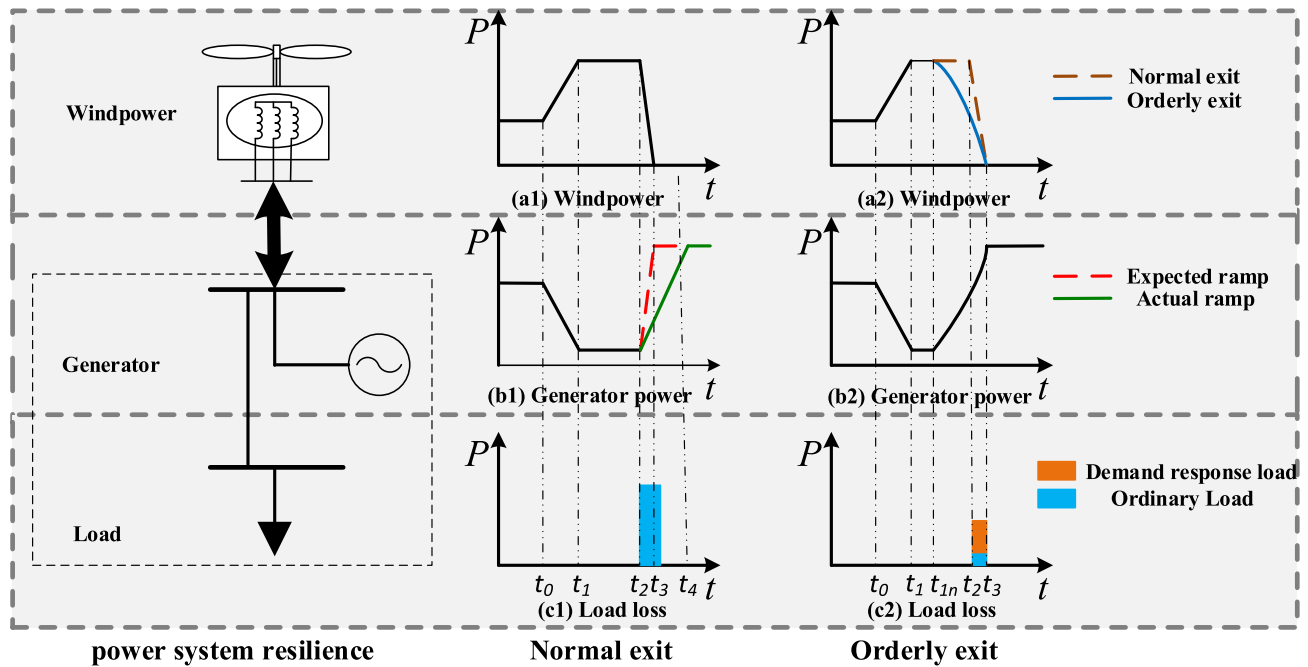


FIGURE 1. Schematic diagram of using the resilience of the grid to cope with wind power ramping.

storage [22]–[24] has achieved good results. Threshold values for the ramp power and the ramp rate are utilized in this method to quantitatively analyze the wind power ramp event to optimize wind power curtailment and energy storage [25], [26]. The above research presents the measures for addressing wind power ramp events using a storage system, focusing on ramping control at the wind farm side and ignoring the changes in the power system's operating state. Therefore, it may not give a reasonable explanation for the fixed threshold values for ramp power and ramp rate when changes in the power system's operating state occur.

The motivation of this paper is to reduce the amount of wind power curtailment and the operation cost of the system when wind power ramp-down events attributed to extreme weather conditions occur. Therefore, in view of the above deficiencies, this paper analyzes the impact of typhoon on the output characteristics of offshore wind power. From the perspective of large-scale power grids, an ordered curtailment strategy for OWPGs considering the resilience of the power grid is proposed to optimize the exit of offshore wind turbines prior to the typhoon's arrival. Based on the optimized exit of the OWPGs, the regulation capabilities of the system's thermal and hydro power units are dispatched in advance, and the response capability of controllable loads is utilized to effectively control the wind power ramping.

This paper is organized as follows: Section II describes the power system resilience for wind power ramping to analyze the regulation capability of the system when wind power ramp events occur. The output characteristics of typhoon-affected offshore wind power are analyzed and the impact of the typhoon on an offshore wind farm is summarized

in Section III. Section IV presents the proposed ordered curtailment strategy for OWPGs. Section V illustrates the simulation results conducted in the IEEE-RTS 24 node test system. Section VI concludes the paper.

II. THE RESILIENCE OF THE GRID FOR WIND POWER RAMPING

The impact of the typhoon on an offshore wind farm is mainly concentrated on the wind power ramp events caused by large-scale wind turbine tripping in a short time after the wind turbine reaches its cut-off wind speed. As shown in Figure 1 (a1), the wind power output reaches the rated power during the period from t_0 to t_1 when the typhoon arrives. After maintaining a constant output for a period of time, the cut-off wind speed is reached at time t_2 , and the wind power quickly exits over a short time, until t_3 . During the period from t_0 to t_1 , the system can adjust the output of the generators to cope with the increased wind power output, maintaining the balance of supply and demand. However, the wind turbines stop operating over the short period of time from t_2 to t_3 . Due to unit ramp rate limitations, the traditional generator output cannot be quickly increased in a short time to ensure the balance of power supply with system consumption. Therefore, the system will deal with the power shortage in the form of load loss.

In fact, during the period from t_2 to t_3 , the generators in the system have sufficient peak-load regulation capability, and the system's power shortage event is caused by the limitation of the unit ramp rate. Therefore, in order to leave sufficient time to allow the system's peak-load regulation capability to reduce the power shortage of the system, the orderly exit of

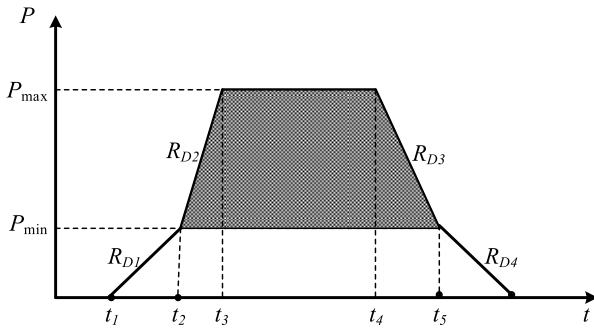


FIGURE 2. The regulation capability of the generator.

wind turbines can be considered prior to reaching the cut-off wind speed, which is shown in Figure 1 (a2). In addition, some loads in the system have active response capability, which can be utilized to reduce the significant load loss in the system when the power shortage event occurs. Therefore, the resilience of the grid to handle wind power ramp events is reflected in the regulation capacity of the generator and the active response capability of the load.

A. The REGULATION CAPABILITY OF GENERATORS

Figure 2 depicts the regulation capability of the generator, which is determined by its rated capacity and ramp rate limitation. Period t_1-t_2 represents the start-up phase, during which the generator does not have regulation ability, indicating that it can only start up according to the ramp rate R_{D1} . Similarly, period t_4-t_5 represents the shut-down phase, in which the generator also does not have adjustment capability. However, the generator can operate at any point in the shadowed area in the operation phase from t_2 to t_4 . However, the output adjustment of the generator is limited by the ramp rate and the rated capacity, which can be expressed as:

$$P_{\min} \leq P \leq P_{\max} \tag{1}$$

$$-R_{D3}\Delta t \leq P_t - P_{t-1} \leq R_{D2}\Delta t \tag{2}$$

where P_{\max} and P_{\min} are the unit’s maximum output and minimum technical output, R_{D2} and R_{D3} are the unit’s ramp rates, and P_t, P_{t-1} represent the generator output at times t and $t-1$, respectively.

Due to large-scale wind turbine tripping in a short period of time when a typhoon arrives, leading to large power shortages over a short period of time, it is necessary for each generator to increase its output. Meanwhile, considering the units’ start-up and shut-down costs, this paper only studies the adjustment ability of units during their operation period.

Nuclear power generally operates as a base load and does not participate in the peak regulation of the power grid. The ramp rate of thermal power units is generally 2%-5% of rated capacity per minute, while hydro power units are faster, reaching 50%-100% of rated capacity per minute. However, thermal power generators account for a large proportion of the power system, so the adjustment ability of the system may be limited by the ramp rate of the thermal power generators.

B. THE RESPONSE CAPABILITY OF LOADS

The utilization of the active response capability of the load [27]–[30], such as air conditioners, water heaters and electric vehicles, has achieved good results in dealing with the active power vacancy in the power grid. The aggregation model is adopted to evaluate the response capability of the load, which can be expressed as:

$$P(t) = \sum_{i=1}^{n_1} S_i(t)P_{AC,i,t} + \sum_{j=1}^{n_2} S_j(t)P_{WH,j,t} + \sum_{k=1}^{n_3} S_k(t)P_{EV,k,t} \tag{3}$$

where $P_{AC,i,t}, P_{WH,j,t}, P_{EV,k,t}$ are the response powers of the air conditioners, water heaters, and electric vehicles, respectively. $S_i(t), S_j(t), S_k(t)$ are the states of the air conditioners, water heaters, and electric vehicles, respectively, at time t , and $n_1, n_2,$ and n_3 represent the number of air conditioners, water heaters, and electric vehicles, respectively.

From Equation (3), we can conclude that the response potential of load aggregators is influenced by the load composition and the response loads’ states. The former is related to the load category and proportion in load aggregators, the latter is determined by user comfort and load response times.

III. THE IMPACT OF THE TYPHOON ON OFFSHORE WIND POWER

This section aims to analyze the wind speed characteristics of an offshore wind farm during typhoon periods, and then study the offshore wind power output characteristics.

A. WIND SPEED CHARACTERISTIC

The Rankine vortex field model [31] has a precise simulation result for typhoons, and it also has high computational efficiency. In this context, this paper models the typhoon adopting the Rankine vortex field model, which can be illustrated as:

$$v_i = \begin{cases} \frac{r_i}{R_{\max}} v_{\max} & r_i \in [0, R_{\max}] \\ \frac{R_{\max}}{r_i} v_{\max} & r_i \in [R_{\max}, \infty) \end{cases} \tag{4}$$

where v_i is the wind speed at position i , v_{\max} is the maximum typhoon wind speed, r_i is the distance from i to the typhoon center, and R_{\max} is the maximum wind speed radius of the typhoon.

In addition, the distance from i to the center of typhoon can be illustrated as:

$$r_i = R * \{\arccos[\cos b * \cos y * \cos(a-x) + \sin b * \sin y]\} \tag{5}$$

where (x, y) and (a, b) are the latitude and longitude coordinates of position i and the typhoon center, respectively (east longitude is positive and north latitude is positive), and R is the earth’s radius, which is 6371 km.

Meanwhile, the maximum wind speed radius of a typhoon can be given by [31]:

$$R_{\max} = 80 - k(950 - P_c) \tag{6}$$



FIGURE 3. The influence of ‘Maria’ on the Fujian Changle offshore wind farm.

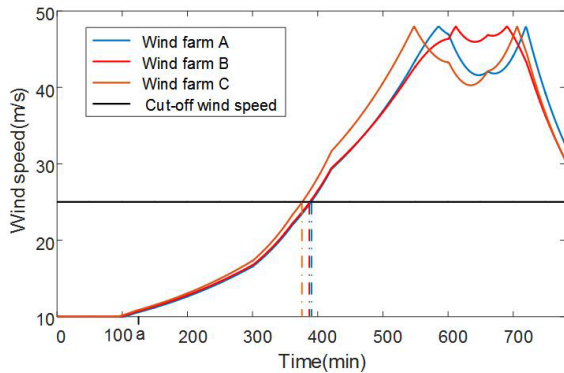


FIGURE 4. Wind speed characteristic in a typhoon condition.

where P_c is the atmospheric pressure around the center of the typhoon, and k is the model coefficient, which is obtained from other researchers’ simulation assessment work and has a value of 0.769.

Taking typhoon “Maria” as an example, this paper analyzes the impact of a typhoon on the Changle offshore wind farm in Fujian province. Figure 3 shows the path of typhoon “Maria” and the position of the Changle offshore wind farm. When the typhoon is close to a wind farm, the wind speed near the wind farm will continue to increase over a short time, and then the wind farm will be cut off as a result of reaching the cut-off wind speed, which will affect the safe and stable operation of the offshore wind power grid-connected system. Therefore, adopting the Rankine vortex model illustrated above, the wind speed at the Changle offshore wind farm can be obtained as depicted in Figure 4, which shows the wind speed in three areas will reach the cut-off wind speed simultaneously.

B. OFFSHORE WIND POWER OUTPUT CHARACTERISTIC

The typhoon has a large impact on the wind speed at the offshore wind farm, which in turn affects its output characteristics and can be described by:

$$P = \begin{cases} 0 & v_{wind} < v_{in}, \quad v_{wind} \geq v_{out} \\ \frac{1}{2} \rho C_p \pi r^2 v_{wind}^3 & v_{in} \leq v_{wind} \leq v_{rate} \\ P_{rate} & v_{rate} < v_{wind} < v_{out} \end{cases} \quad (7)$$

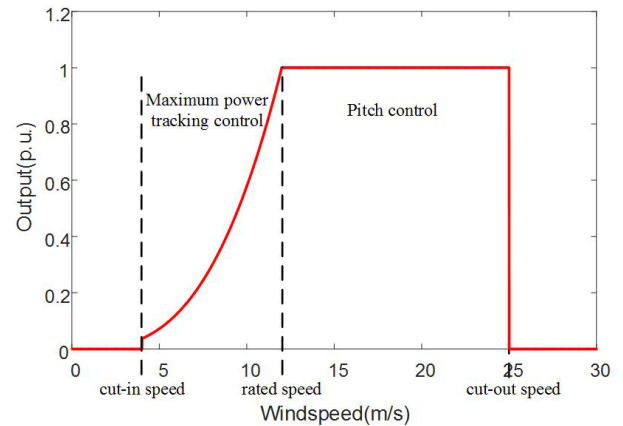


FIGURE 5. The relationship between the output of wind turbine and the wind speed.

where ρ denotes air density; C_p represents the aerodynamic performance function, which is related to the wind turbine’s tip speed ratio and pitch angle; r is the blade radius; v_{wind} is the wind speed; and v_{in} , v_{rate} , v_{out} are the cut-in, rated, and cut-off wind speeds, respectively. P_{rate} is the rated output of the wind turbine. Figure 5 depicts the relationship between the output of the wind turbine and the wind speed.

From Figure 4, we can see that the wind speed in three areas of the Changle offshore wind farm will reach the cut-off wind speed simultaneously, especially A and B. On this basis, the output characteristic in a typhoon condition has been obtained, as shown in Figure 6, in which the wind power is reduced from the rated value to zero in 25 minutes. This situation presents the problem of how to deal with the large power shortage on small time scale, which can be solved by scheduling active offshore wind power curtailment prior to the typhoon, hence prolonging the duration of wind power exit and reducing the power change rate. However, premature curtailment of the wind power induces large economic losses. Meanwhile, the resilience of the grid is also not fully utilized. In this context, this paper proposes an ordered curtailment strategy for offshore wind power in Section IV.

IV. ORDERED CURTAILMENT STRATEGY FOR WIND POWER

As seen from the analysis in Section II, a large number of offshore wind turbines will exit in a short time when the typhoon arrives. However, the thermal units’ ramp rate is limited, making it difficult to immediately make up for the large power shortage of the system. Also, the demand response in the system is quite limited. Therefore, it is necessary to power down the offshore wind turbines in advance to avoid the occurrence of a significant load loss due to a short-term large power shortage in the system.

A. OBJECTIVE FUNCTION

The goal of ordered curtailment for offshore wind power is to optimize the exit of offshore wind power before the arrival

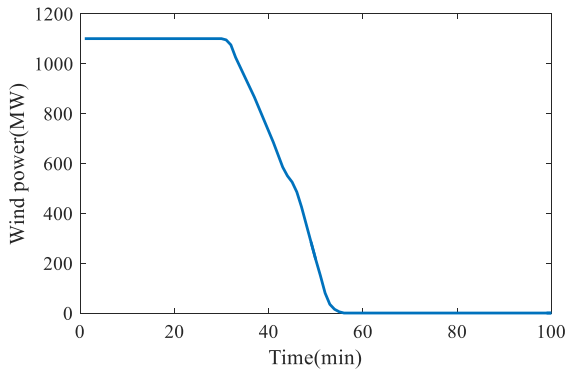


FIGURE 6. Output characteristic in a typhoon condition.

of a typhoon, to minimize the operating cost and load loss of the system. The objective function can be expressed as:

$$\min \sum_T (C_w P_{w,loss,t} + \sum_k^{NG} C_g P_{g,k,t} + \sum_n^N C_l P_{loss,n,t} + \sum_j^{NL} C_d P_{d,j,t}) \quad (8)$$

where C_w, C_g, C_l, C_d are the cost of wind curtailment, generator operation, load loss, and demand response, respectively. $P_{W,loss,t}$ is the amount of wind curtailment at time t . Similarly, $P_{g,k,t}$ is the output of generator k at time t , $P_{loss,n,t}$ is the load loss at bus n , and $P_{d,j,t}$ is the response quality of the demand respond load j at time t . NG, N, NL are the number of generators, nodes, and responding loads. T is the total scheduling time.

B. CONSTRAINTS

1) ACTIVE POWER BALANCE CONSTRAINTS

$$\sum_{i \in \delta^-(n)} L_{i,t} - \sum_{i \in \delta^+(n)} L_{i,t} + \sum_k^{NG} P_{g,k,t} + P_{w,t} + \sum_j^{NL} P_{d,j,t} + \sum_n^N P_{loss,n,t} - P_{w,loss,t} = \sum_n^N D_{n,t} \quad (9)$$

where $L_{i,t}$ is the transmission power through line i at time t , and δ_n^+, δ_n^- are lines specified at node n as front and terminal, respectively. $P_{w,t}$ is the wind power output at time t , and $D_{n,t}$ is the load connected to bus n at time t .

2) POWER FLOW CONSTRAINTS

$$P_{pq,t} = B_{pq}(\theta_{p,t} - \theta_{q,t}) \quad (10)$$

where $P_{pq,t}$ is the transmission power through line specified p, q as the endpoint at time t . B_{pq} is the line susceptance, and $\theta_{p,t}, \theta_{q,t}$ are the phase angles of the p and q nodes at time t .

3) GENERATOR OUTPUT CONSTRAINTS

$$P_{g,k,t} - rsv_{g,k,t}^D \geq P_{g,k,min} \quad (11)$$

$$P_{g,k,t} + rsv_{g,k,t}^U \leq P_{g,k,max} \quad (12)$$

where $P_{g,k,min}, P_{g,k,max}$ are the minimum technical output and the maximum output of generator k , and $rsv_{g,k,t}^U, rsv_{g,k,t}^D$ are the positive and negative reserve capacities of generator k at time t .

4) GENERATOR RAMP RATE CONSTRAINTS

$$R_{d,k,t} \Delta t \leq P_{g,k,t} - P_{g,k,t-1} \leq R_{u,k,t} \Delta t \quad (13)$$

where $R_{d,k,t}, R_{u,k,t}$ are the up and down ramp rates of generator k at time t , $P_{g,k,t}, P_{g,k,t-1}$ are the outputs of generator k at times t and $t-1$, and Δt is the time interval.

5) GENERATOR RESERVE CONSTRAINTS

The reserve capacity constraint and reserve response rate constraint are included in the generator reserve constraints, which can be expressed as:

$$\begin{cases} \sum_{k=1}^{NG} rsv_{g,k,t}^U \geq rsv_{req}^U \\ \sum_{k=1}^{NG} rsv_{g,k,t}^D \geq rsv_{req}^D \end{cases} \quad (14)$$

where rsv_{req}^U, rsv_{req}^D are the reserve capacities required by the system.

In addition, the reserve response rate is also subject to the unit's ramp rate.

6) LINE TRANSMISSION LIMIT CONSTRAINTS

$$|P_{pq,t}| \leq P_{pq,lim} \quad (15)$$

where $P_{pq,lim}$ is the transmission power limit of line pq .

7) PHASE ANGLE CONSTRAINTS

$$-\pi \leq \theta_{n,t} \leq \pi \quad (16)$$

where $\theta_{n,t}$ is the phase angle of node n at time t .

8) WIND CURTAILMENT CONSTRAINTS

$$0 \leq P_{wind} \times N_{w,loss,t} \leq P_{sum,wind} \quad (17)$$

$$\sum_{t=1}^{T_n} N_{w,loss,t} = N_{sum,wind} \quad (18)$$

where P_{wind} is the rated capacity of a single wind turbine, $P_{sum,wind}$ is total installed wind power capacity, $N_{w,loss,t}, N_{sum,wind}$ are the number of abandoned wind turbines at time t and the total number of wind turbines, respectively, and T_n is the time at which the offshore wind farm reached the cut-off wind speed.

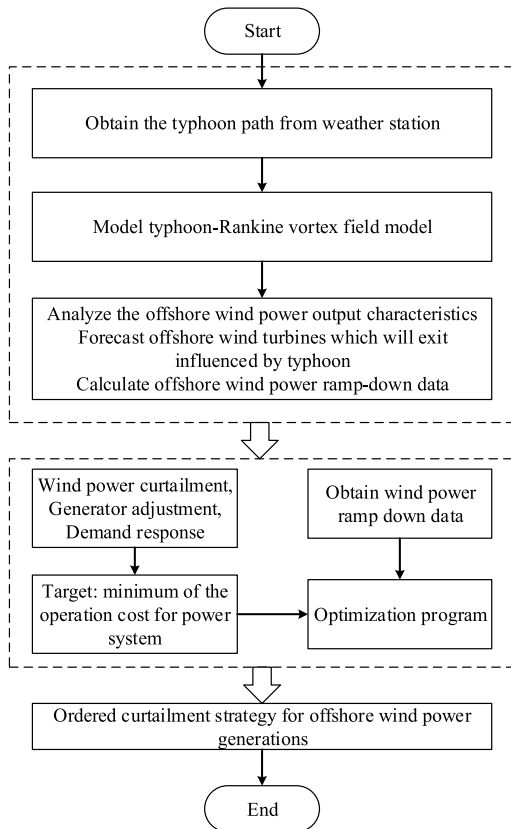


FIGURE 7. Overall framework of the proposed strategy.

9) DEMAND RESPONSE POTENTIAL CONSTRAINTS

$$0 \leq P_{d,j,t} \leq P_{d,j,t,lim} \tag{19}$$

where $P_{d,j,t,lim}$ is the response potential of load aggregator j at time t .

10) LOAD LOSS CONSTRAINTS

$$0 \leq P_{loss,n,t} \leq D_{n,t} \tag{20}$$

where $D_{n,t}$ is the rated capacity of the load connected at bus n at time t .

C. OPTIMIZATION RESULTS

The above optimization model is solved with MATLAB optimization toolbox “linprog”. Moreover, the results obtained by solving the above optimization model represent the ordered curtailment strategy for offshore wind power before the arrival of a typhoon and provide the dispatching department with an output reference for generator units.

D. Overall framework

The overall framework of the proposed ordered curtailment strategy for offshore wind power under extreme weather conditions is depicted in Figure 7. The aim of the proposed strategy is to reduce the wind power curtailment and minimize the

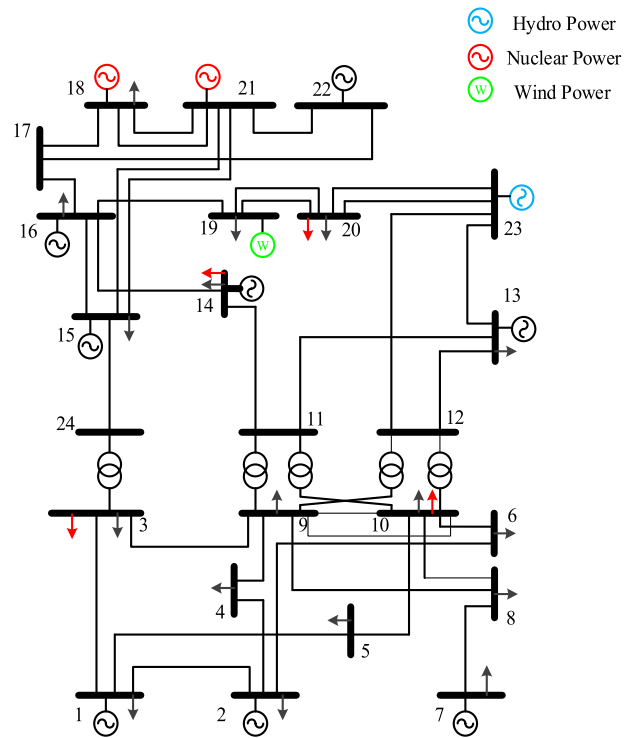


FIGURE 8. Study system.

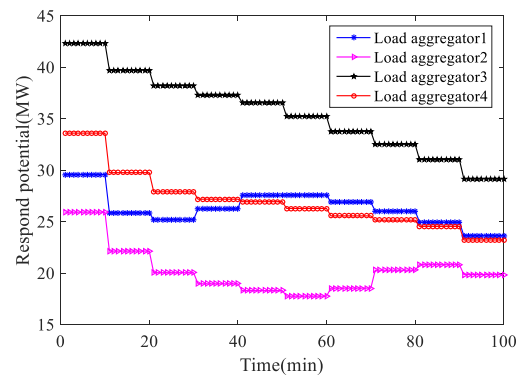


FIGURE 9. Response potential of load aggregators.

system’s operation cost when wind power ramp-down events caused by extreme weather occur. When extreme weather such as typhoon exists, the Rankine vortex field model will be set up adopting the data obtained from weather station. Furthermore, the offshore wind power output characteristics will be analyzed and the offshore wind power ramp-down data will be calculated.

After obtaining wind power ramp-down data, the minimum of the operation cost for power system is achieved by determining the wind power curtailment, adjustment ability of the generator, and demand response capability. The ordered curtailment strategy for offshore wind power can be obtained by solving the optimization model.

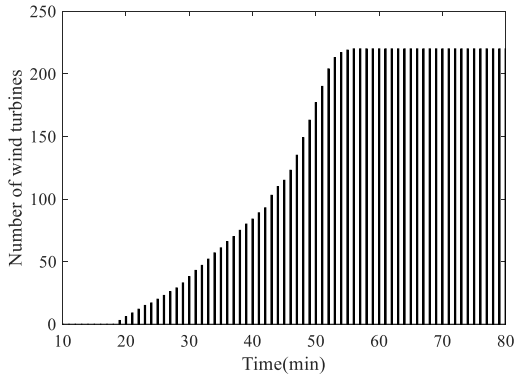


FIGURE 10. Orderly curtailment strategy for offshore wind power.

TABLE 1. Generator costs.

Series number	Node number	Cost of generator (\$/MWh)
1	1	11.46
2	2	11.46
3	7	18.60
4	13	19.20
5	14	0
6	15	9.92
7	16	9.92
8	18	5.31
9	21	5.31
10	22	0
11	23	10.08

TABLE 2. Demand response costs.

Series number	Node number	Cost of demand response (\$/MWh)
1	3	14.18
2	10	13.18
3	14	12.11
4	20	13.16

V. CASE STUDY

The simulation results for the proposed strategy are carried out in this section based on the IEEE-RTS 24 node test system, which contains 24 nodes and 38 transmission lines. The total load of the system is 2850 MW, while the maximum output of the generators is 3450 MW. As illustrated in Figure 8, the Changle offshore wind farm with a capacity of 1100 MW is connected to bus 19, while the nuclear power units and hydro power units are connected to buses 18, 21, and 23, respectively. Additionally, the response loads are connected to buses 3, 10, 14, and 20, and their response potentials are described in Figure 9.

Tables 1 and 2 describe the cost of each generator and the demand response, respectively. The cost of wind curtailment is \$21 per MWh. To minimize the probability of load loss, the cost of load loss is set to \$1000 per MWh. Moreover, the ramp rate of each generator is shown in Table 3.

TABLE 3. Generator ramp rates.

Series number	Node number	Ramp rate of generator (MW/min)
1	1	1.92
2	2	1.92
3	7	3.00
4	13	5.91
5	14	0
6	15	2.15
7	16	1.55
8	18	0
9	21	0
10	22	150.00
11	23	6.60

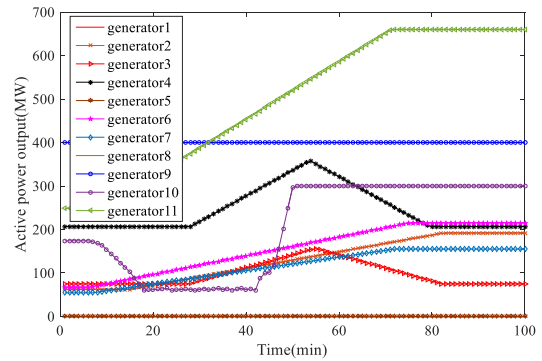


FIGURE 11. Generator output in the wind power ordered curtailment strategy.

A. ORDERED CURTAILMENT STRATEGY FOR WIND POWER

Figure 10 depicts the ordered curtailment strategy for offshore wind power obtained by the model proposed in Section III. The Changle offshore wind farm is affected by a typhoon at 30 min with a duration of 26 min. The wind turbines start to exit at 19 min, and significant load loss does not occur in the system.

Figures 11 and 12 illustrate the output of each generator set and the response of each load aggregator in this process. Due to the early exit of the wind turbines and the faster adjustment of the hydro power unit, the hydro power will reduce its output before the typhoon comes, leaving enough time for the thermal power units to increase their output, so that wind power ramping can be suppressed effectively. Moreover, the rapid adjustment capability of the hydro power units and the response capacity of the load aggregators are utilized to compensate for the short-term power shortage of the system during the period of wind power ramping caused by the typhoon.

Additionally, after the offshore wind power is cut off, load aggregators continue to respond, while generators 3 and 4 reduce their output due to high operating costs, making the system operate more economically, as shown in Figure 12.

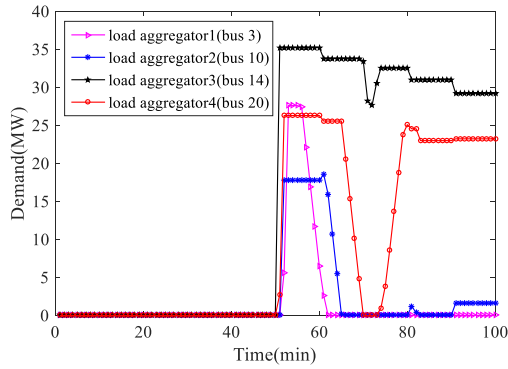


FIGURE 12. Demand response in the wind power ordered curtailment strategy.

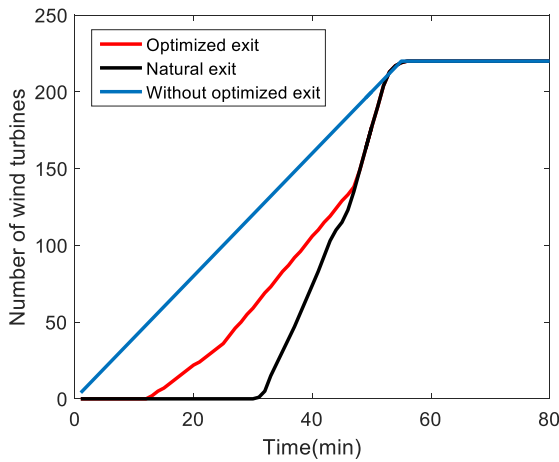


FIGURE 13. A comparison of three exit strategies for offshore wind power.

B. THE VALIDITY ANALYSIS OF THE METHOD

The offshore wind power clusters in the A, B and C areas of the Fujian Changle offshore wind farm will all exit within 26 minutes when affected by typhoon “Maria”, as shown by the black line in Figure 13. To comprehensively check the validity of the proposed strategy, the following 3 exit strategies for wind power are considered.

Strategy 1: Offshore wind turbines naturally exit when reaching the cut-off wind speed.

Strategy 2: Offshore wind turbines begin to exit 30 minutes before their natural exit (the same number of wind turbines per minute exit).

Strategy 3 (Strategy Proposed in This Paper): The wind curtailment cost, generator operation cost, load response cost, and load loss cost are comprehensively considered to optimize the ordered curtailment for wind turbines to release the adjustment capability of the generators in advance.

Table 4 illustrates the scheduling results obtained by the above exit strategies for wind turbines. Strategy 1 cannot guarantee the security and stability of power system operation since significant load loss in the period of 44-68min

TABLE 4. Scheduling results under different strategies.

Strategy	System operation cost (\$)	Load loss period (min)
Strategy 1	\	44-68
Strategy 2	65521.22	none
Strategy 3	61203.12	none

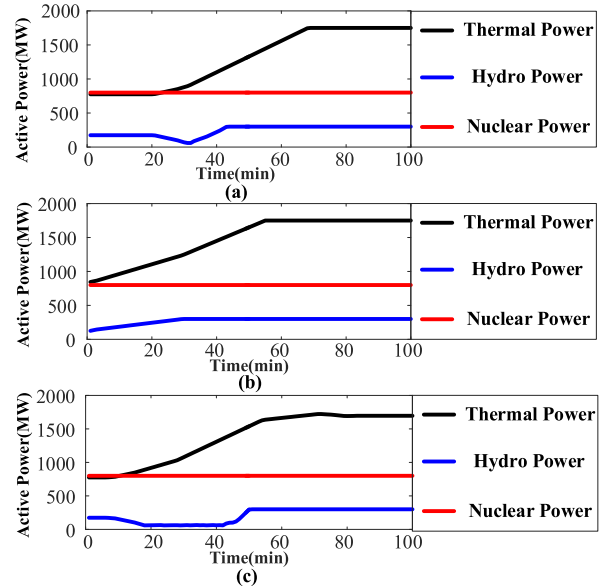


FIGURE 14. The output of generators in three strategies.

occurs. Moreover, load loss can be avoided when strategy 2 is adopted. However, the high operation cost is inevitable. That means if the offshore wind turbines do not exit in advance, load loss will occur in the system, while without the optimized wind turbines exit, it is difficult to guarantee the economics of the system operation. As shown in Table 4, considering the ordered curtailment of wind power, the optimized and ordered curtailment strategy for wind turbines described in this paper can improve the economics of system operation under the premise of ensuring the security and stability of power system operation.

The output of generators in three strategies is illustrated in Figure 14. Compared with strategy 1, the proposed optimized and orderly exit strategy can schedule the adjustment ability of the thermal and hydro power units in advance, avoiding the short-term large power shortage of the system, which may cause significant load loss. Due to the earlier exit of the wind turbines in strategy 2, each thermal power unit has enough time to increase its output and is not limited by its ramp rate. However, the rapid adjustment capability of the hydro power unit and the responsiveness of the demand response are not fully utilized. Although the safety of the system can be ensured, the operating cost of the system will increase because of the premature wind curtailment.

VI. CONCLUSION

This paper has developed an ordered curtailment strategy for offshore wind power considering the resilience of the grid. We draw the following conclusions on the basis of research on offshore wind power ramp events:

(1) Offshore wind power ramping caused by typhoons may seriously threaten the safe and stable operation of the power system;

(2) The proposed ordered curtailment strategy for offshore wind power can effectively utilize the adjustment ability of the system, avoiding the influence of brief, severe shortages of wind power ramp events on the balance of supply and demand.

(3) The proposed strategy reduces the operation cost of the system as much as possible while guaranteeing the security and stability of the power system's operation.

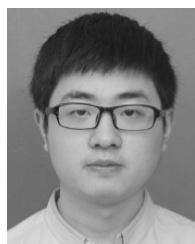
REFERENCES

- [1] S. Tao, X. Zhang, Y. Wang, and J. Yang, "Transient behavior analysis of offshore wind turbines during lightning strike to multi-blade," *IEEE Access*, vol. 6, no. 1, pp. 22070–22083, Apr. 2018.
- [2] S.-Z. Chen *et al.*, "An aerodynamics-based novel optimal power extraction strategy for offshore wind farms with central VSCs," *IEEE Access*, vol. 6, pp. 44351–44361, Dec. 2018.
- [3] P. Hou, W. Hu, M. Soltani, C. Chen, B. Zhang, and Z. Chen, "Offshore wind farm layout design considering optimized power dispatch strategy," *IEEE Trans. Sustain. Energy*, vol. 8, no. 2, pp. 638–647, Apr. 2017.
- [4] M. Saruwatari *et al.*, "Design study of 15-MW fully superconducting generators for offshore wind turbine," *IEEE Trans. Appl. Supercond.*, vol. 26, no. 4, pp. 1–5, Jun. 2016.
- [5] I. Erlich, F. Shewarega, C. Feltes, F. W. Koch, and J. Fortmann, "Offshore wind power generation technologies," *Proc. IEEE*, vol. 101, no. 4, pp. 891–905, Apr. 2013.
- [6] Y. Fujimoto, Y. Takahashi, and Y. Hayashi, "Alerting to rare large-scale ramp events in wind power generation," *IEEE Trans. Sustain. Energy*, vol. 10, no. 1, pp. 55–65, Jan. 2019.
- [7] A. Couto, P. Costa, L. Rodrigues, V. V. Lopes, and A. Estanqueiro, "Impact of weather regimes on the wind power ramp forecast in Portugal," *IEEE Trans. Sustain. Energy*, vol. 6, no. 3, pp. 934–942, Jul. 2015.
- [8] Y. Xiong, X. Zha, L. Qin, T. Ouyang, and T. Xia, "Research on wind power ramp events prediction based on strongly convective weather classification," *IET Renew. Power Gener.*, vol. 11, no. 8, pp. 1278–1285, Jun. 2016.
- [9] Y. Gong, C. Y. Chung, and R. S. Mall, "Power system operational adequacy evaluation with wind power ramp limits," *IEEE Trans. Power Syst.*, vol. 33, no. 3, pp. 2706–2716, May 2018.
- [10] G. Morales-España, R. Baldick, J. García-González, and A. Ramos, "Power-capacity and ramp-capability reserves for wind integration in power-based UC," *IEEE Trans. Sustain. Energy*, vol. 7, no. 2, pp. 614–624, Apr. 2016.
- [11] H. Ma, C. Li, and Y. Liu, "Assessing impact of wind power ramp events on operation adequacy of power systems," *Autom. Electr. Power Syst.*, vol. 41, no. 4, pp. 41–47, Feb. 2017.
- [12] Z. Li, L. Ye, Y. Zhao, X. Song, J. Teng, and J. Jin, "Short-term wind power prediction based on extreme learning machine with error correction," *Protection Control Mod. Power Syst.*, vol. 1, no. 1, p. 1, Dec. 2016.
- [13] Y. Qi and Y. Liu, "Wind power ramping control using competitive game," *IEEE Trans. Sustain. Energy*, vol. 7, no. 4, pp. 1516–1524, Oct. 2016.
- [14] M. Cui, J. Zhang, A. R. Florita, B.-M. Hodge, D. Ke, and Y. Sun, "An optimized swinging door algorithm for identifying wind ramping events," *IEEE Trans. Sustain. Energy*, vol. 7, no. 1, pp. 150–162, Jan. 2016.
- [15] T. Ouyang, X. Zha, L. Qin, and A. Kusiak, "Optimization of time window size for wind power ramps prediction," *IET Renew. Power Gener.*, vol. 11, no. 8, pp. 1270–1277, Aug. 2016.
- [16] R. Sevlian and R. Rajagopal, "Detection and statistics of wind power ramps," *IEEE Trans. Power Syst.*, vol. 28, no. 4, pp. 3610–3620, Nov. 2013.
- [17] D. Ganger, J. Zhang, and V. Vittal, "Statistical characterization of wind power ramps via extreme value analysis," *IEEE Trans. Power Syst.*, vol. 29, no. 6, pp. 3118–3119, Nov. 2014.
- [18] Y. Cao, W. Wei, C. Wang, S. Mei, S. Huang, and X. Zhang, "Probabilistic estimation of wind power ramp events: A data-driven optimization approach," *IEEE Access*, vol. 7, pp. 23261–23269, Mar. 2019.
- [19] M. Cui, D. Ke, Y. Sun, D. Gan, J. Zhang, and B. M. Hodge, "Wind power ramp event forecasting using a stochastic scenario generation method," *IEEE Trans. Sustain. Energy*, vol. 6, no. 2, pp. 422–433, Apr. 2015.
- [20] B. Du *et al.*, "Finite control strategy for wind power ramping based on segmentation optimization," *Autom. Electr. Power Syst.*, vol. 40, no. 5, pp. 78–82, Mar. 2016.
- [21] Y. Qi and Y. Liu, "Finite control of high risk wind power ramping," *Proc. CSEE*, vol. 33, no. 13, pp. 69–74, May 2013.
- [22] Y. Gong, Q. Jiang, and R. Baldick, "Ramp event forecast based wind power ramp control with energy storage system," *IEEE Trans. Power Syst.*, vol. 31, no. 3, pp. 1831–1844, May 2016.
- [23] S. Teleke, M. E. Baran, S. Bhattacharya, and A. Huang, "Validation of battery energy storage control for wind farm dispatching," in *Proc. IEEE PES Gen. Meeting*, Jul. 2010, pp. 1–7.
- [24] T. K. A. Brekken, A. Yokochi, A. von Jouanne, Z. Z. Yen, H. M. Hapke, and D. A. Halamaj, "Optimal energy storage sizing and control for wind power applications," *IEEE Trans. Sustain. Energy*, vol. 2, no. 1, pp. 69–77, Jan. 2011.
- [25] L. S. Vargas, G. Bustos-Turu, and F. Larraín, "Wind power curtailment and energy storage in transmission congestion management considering power plants ramp rates," *IEEE Trans. Power Syst.*, vol. 30, no. 5, pp. 2498–2506, Sep. 2015.
- [26] D. Lee, J. Kim, and R. Baldick, "Stochastic optimal control of the storage system to limit ramp rates of wind power output," *IEEE Trans. Smart Grid*, vol. 4, no. 4, pp. 2256–2265, Dec. 2013.
- [27] N. G. Paterakis, O. Erdiç, and J. P. S. Catalão, "An overview of demand response: Key-elements and international experience," *Renew. Sustain. Energy Rev.*, vol. 69, pp. 871–891, Mar. 2016.
- [28] C. Eksin, H. Deriç, and A. Ribeiro, "Demand response management in smart grids with heterogeneous consumer preferences," *IEEE Trans. Smart Grid*, vol. 6, no. 6, pp. 3082–3094, Nov. 2015.
- [29] J. Feng, B. Zeng, D. Zhao, G. Wu, Z. Liu, and J. Zhang, "Evaluating demand response impacts on capacity credit of renewable distributed generation in smart distribution systems," *IEEE Access*, vol. 6, pp. 14307–14317, Sep. 2017.
- [30] M. Shafie-Khah, P. Siano, and J. P. S. Catalão, "Optimal demand response strategies to mitigate oligopolistic behavior of generation companies using a multi-objective decision analysis," *IEEE Trans. Power Syst.*, vol. 33, no. 4, pp. 4264–4274, Jul. 2018.
- [31] A. C. Phadke, C. D. Martino, K. F. Cheung, and S. H. Houston, "Modeling of tropical cyclone winds and waves for emergency management," *Ocean Eng.*, vol. 30, no. 4, pp. 553–578, 2003.



QI WANG (S'13–M'17) received the bachelor's, master's, and Ph.D. degrees in electrical engineering from Southeast University, Nanjing, China, in 2010, 2012, and 2016, respectively, where he is currently a Lecturer with the School of Electrical Engineering.

His research interests include power system stability and control, and cyber physical power systems.



ZHIPENG YU received the bachelor's degree from the Hefei University of Technology, Hefei, China, in 2017. He is currently pursuing the M.S. degree with Southeast University, Nanjing, China.

His current research interests include power system operation and control, and power electronics dominated power systems.



RONG YE received the B.E. degree from Central South University, China, in 2007, and the Ph.D. degree from the South China University of Technology, China, in 2013.

Since 2013, he has been with the State Grid Fujian Economic Research Institute, Fuzhou, China. His main research interests include renewable energy systems and power system planning.



YI TANG (M'07–SM'19) received the Ph.D. degree from the Harbin Institute of Technology, Harbin, China, in 2006.

He is currently an Associate Professor with Southeast University, Nanjing, China. His research interests include smart grid, power system security, power system stability analysis, renewable energy systems, and cyber physical systems.

...



ZHANGSUI LIN received the B.E. degree from Southeast University, China, in 1985, and the M.S. degree from North China Electric Power University, China, in 1990.

He is currently with the State Grid Fujian Economic Research Institute, Fuzhou, China. His main research interests include renewable energy systems and power system planning.